Supplementary Information

Highly Oxygen Deficient and Face Centered Cubic $Pr_3ZrO_{8-\delta}$ as a New Redox Material for Intermediate Temperature Thermochemical Productions of Oxygen and Hydrogen

Jiaxin Lu[a], Yongliang Zhang[a], Luhong Chen [b], Yan Chen [c], Xueling Lei [b]*, Kevin Huang [a]*

[a] Department of Mechanical Engineering, University of South Carolina, Columbia, SC 29201, USA

[b] Department of Physics, Jiangxi Normal University, Nanchang, Jiangxi 330022, China.

[c] Neutron Scattering Division, Oak Ridge National Laboratory, Oak Ridge, TN 37831, USA

* Corresponding authors: huang46@cec.sc.edu; xueling@jxnu.edu.cn.

Table S1. Temperature dependent unit cell parameter, atomic positions, site occupancies, thermal displacement factors and reliable factors of PZO collected in argon

Parameter	**RT**	**300 ºC**	**500 ºC**	**700 ºC**	**900 ºC**
Space group	$Fm\bar{3}m$	$Fm\bar{3}m$	$Fm\bar{3}m$	$Fm\bar{3}m$	$Fm\bar{3}m$
a (Å)	5.43	5.48	5.50	5.52	5.55
V (Å^3)	160.34	164.57	166.38	168.19	170.95
	Pr/Zr (0, 0, 0)				
100 x U_{iso} (Å^2)	1.31	1.51	1.91	2.23	2.57
f_{occ}	0.75/0.25	0.75/0.25	0.75/0.25	0.75/0.25	0.75/0.25
	O (¼, ¼, ¼)				
100 x U_{iso} (Å^2)	4.31	4.83	5.60	6.21	6.54
f_{occ}	0.915	0.910	0.880	0.870	0.860
Reliability Factors					
R_{wp} (%)	4.02	4.09	3.97	3.89	3.46
R_p (%)	3.12	3.21	2.93	2.76	2.69
R_{Brgg} (%)	3.73	3.69	3.65	3.62	3.54
c^2	1.93	1.77	1.74	1.68	1.53

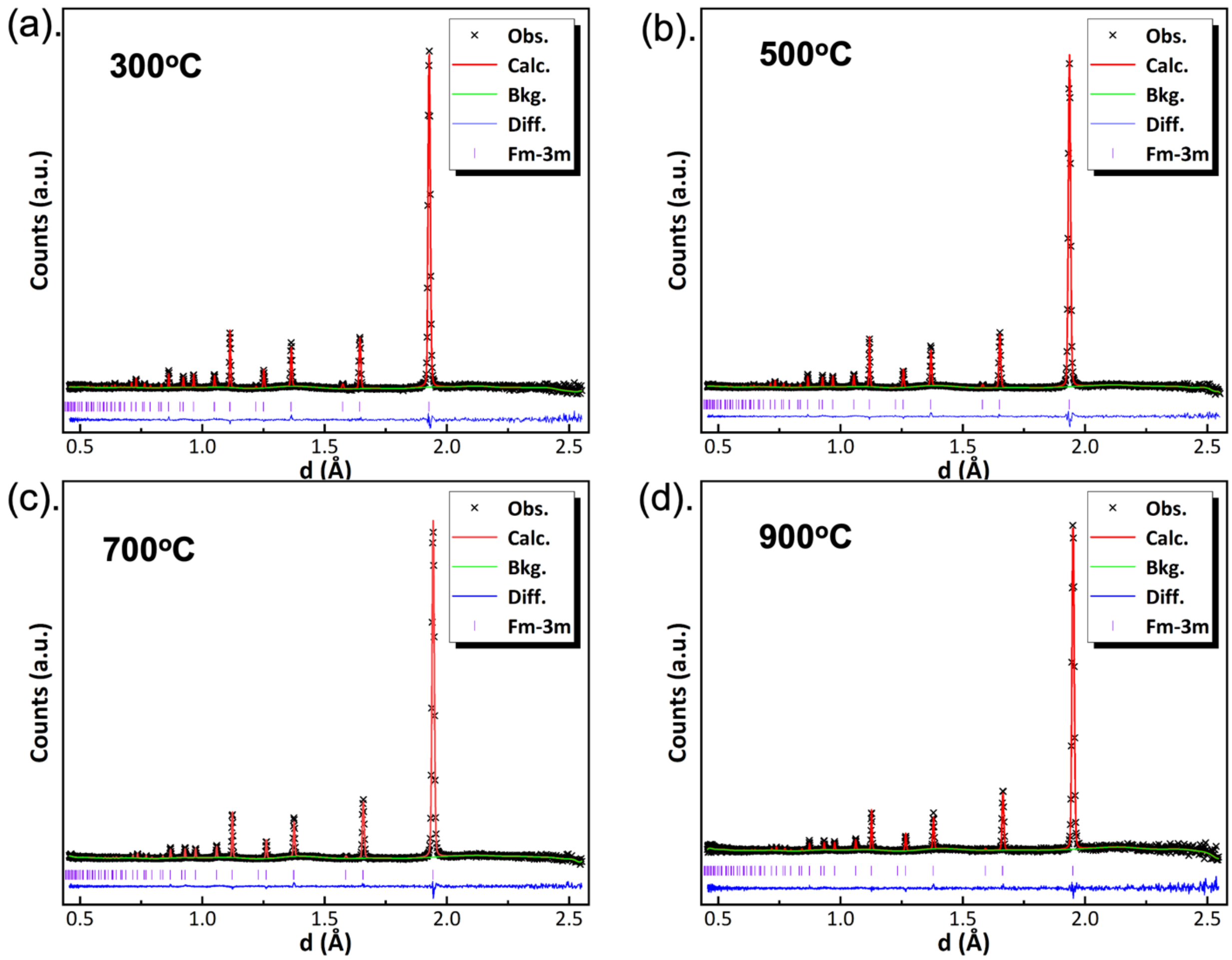

Figure S1. VTND Rietveld refinement profiles of PZO vs. temperatures in argon.

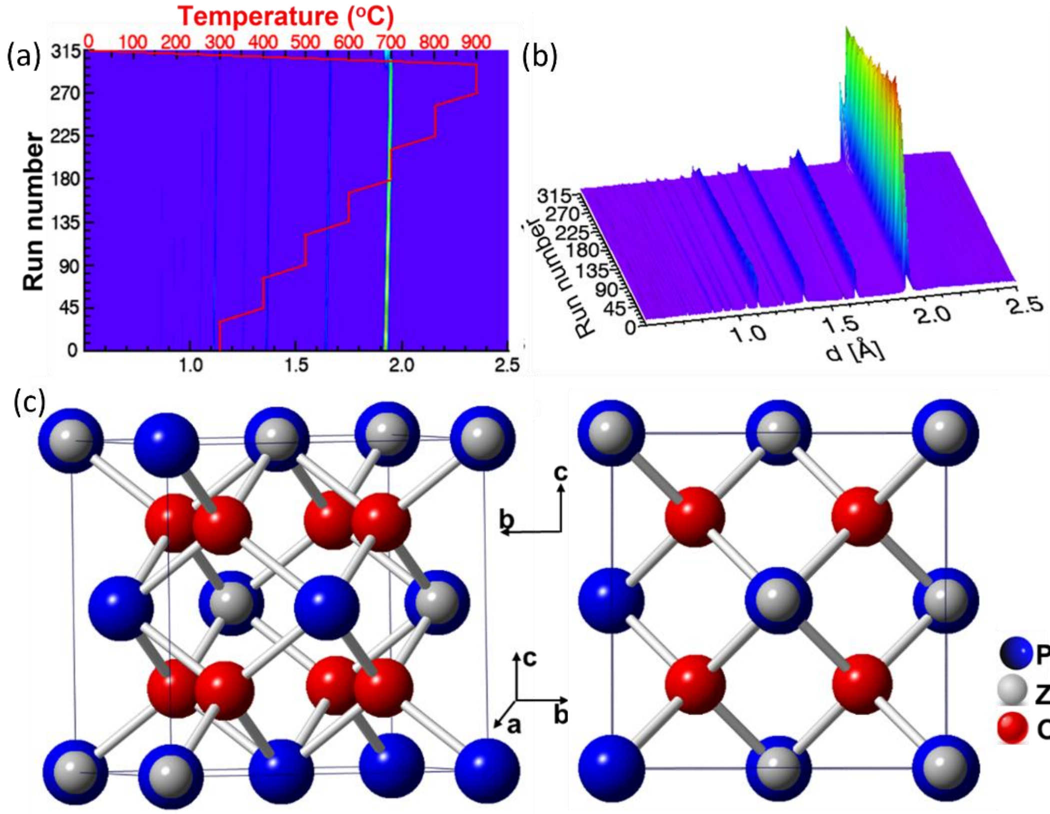

Figure S2. The 2D (a) and 3D (b) intensity contour plots of VTND during heating and cooling in air and (c) the refined crystal structure at room temperature.

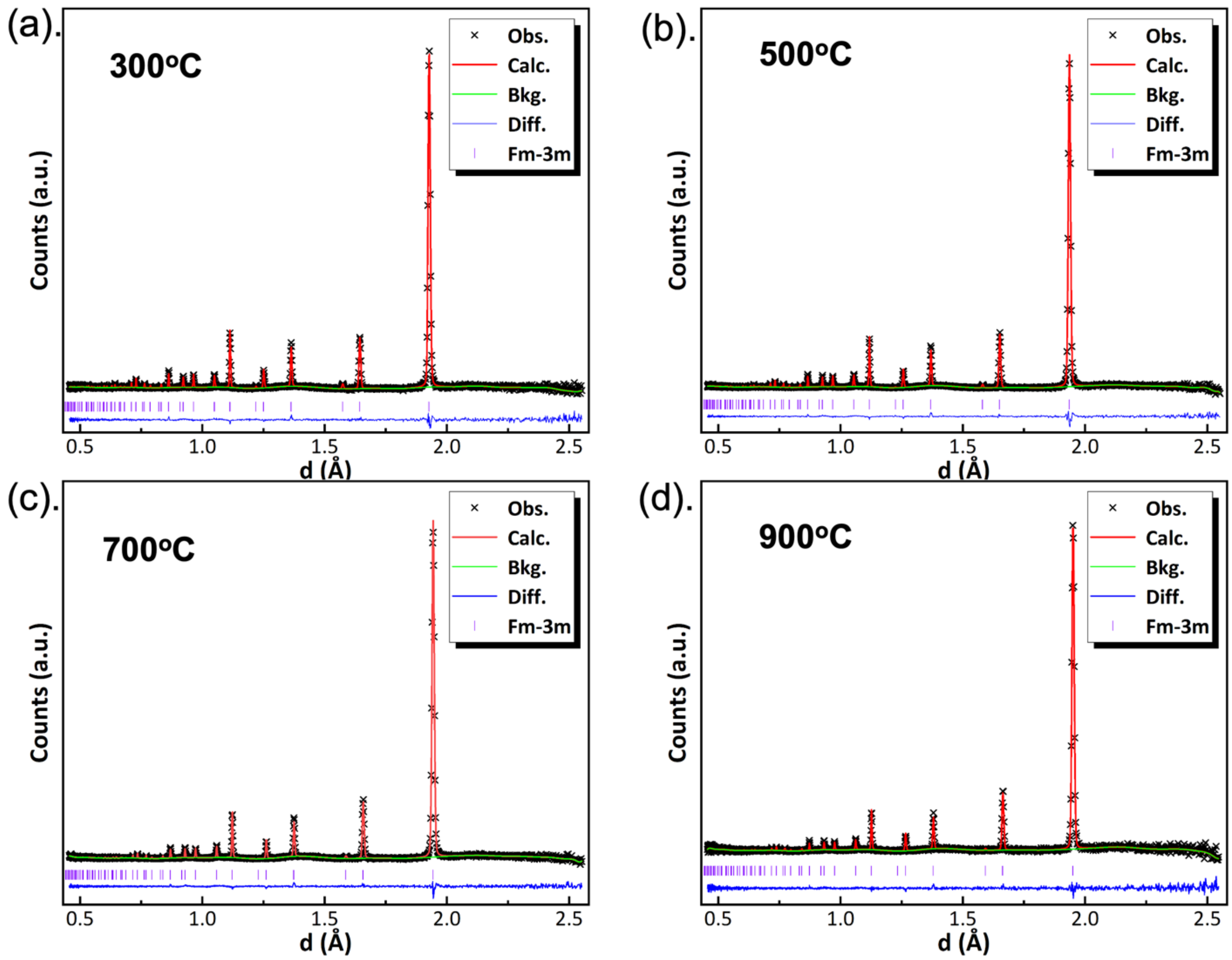

Figure S3. VTND Rietveld refinement profiles of PZO vs. temperatures in air.

Table S2. Temperature dependent unit cell parameter, atomic positions, site occupancies, thermal displacement factors and reliable factors of PZO collected in air.

Parameter	**RT**	**300 ^{o}C**	**500 ^{o}C**	**700 ^{o}C**	**900 ^{o}C**
Space group	Fm-3m	Fm-3m	Fm-3m	Fm-3m	Fm-3m
a (Å)	5.43	5.45	5.47	5.50	5.51
V (Å^3)	160.34	161.92	163.98	165.93	167.72
	Pr/Zr (0, 0, 0)				
100 x U_{iso} (Å^2)	1.213	1.49	1.86	2.21	2.60
f_{occ}	0.75/0.25	0.75/0.25	0.75/0.25	0.75/0.25	0.75/0.25
	O (¼, ¼, ¼)				
100 x U_{iso} (Å^2)	4.31	4.83	5.60	6.21	6.54
f_{occ}	0.915	0.91	0.90	0.89	0.87
Reliability Factors					
R_{wp} (%)	4.20	4.19	4.07	3.66	3.55
R_p (%)	3.32	3.23	3.17	2.87	2.73
R_{Brgg} (%)	3.96	4.03	3.99	3.52	3.76
c^2	2.06	4.10	3.50	2.58	2.01

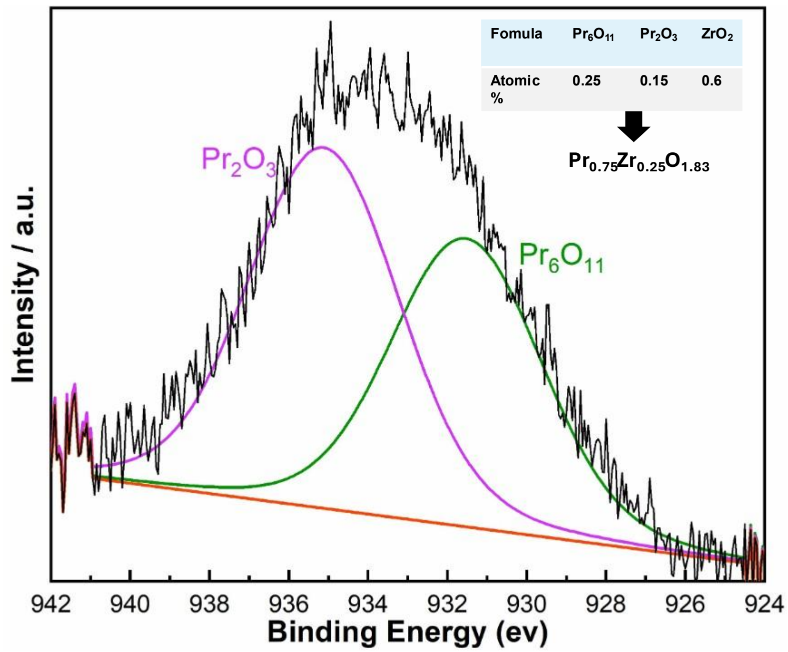

Figure S4. XPS spectrum of the pristine PZO measured at RT.

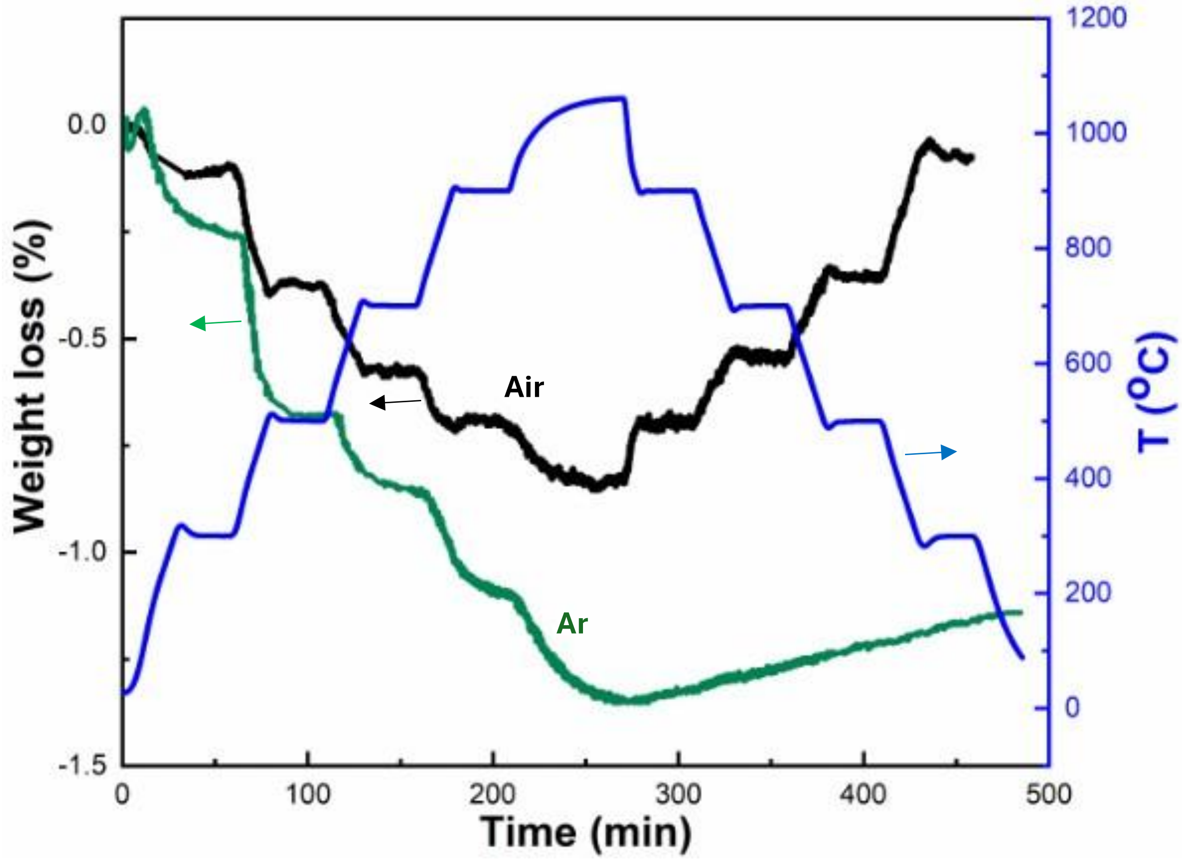

Figure S5. Temperature-dependent TGA profiles measured in air and argon.

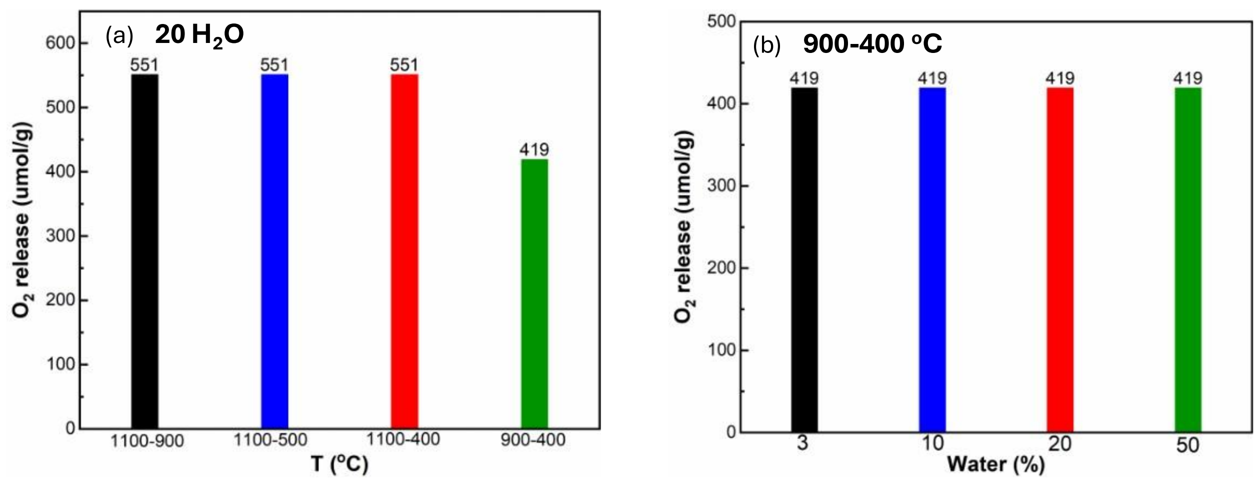

Figure S6. Oxygen yields under (a) different T-window and 20%H_2O (b) different H_2O content and 900-400°C window.

Table S3. Performance comparison of PZO with other RAO materials.

materials	synthesis method	cycles	T(°C) red./ ox.	H_2O (%vol)	Gas red./ox.	O_2 yield (umol/g)	H_2 yield (umol/g)	ref
PZO	sol-gel	10	900/400	20.0	Ar/wet Ar	415.8	85.3	This work
CeO_2	commercial	1	1500/1000	82.0	Ar/wet Ar	49.5	33.8	[1]
CeO_2-Fe_2O_3	commercial	1	1500/1000	82.0	Ar/wet Ar	150.2	86.6	[1]
CeO_2-CuO	commercial	1	1500/1000	82.0	Ar/wet Ar	69.4	43.5	[1]
$LaMnO_{3-d}$	Pechini	3	1350/1000	84.0	N_2/wet N_2	112.8	68.1	[2]
$BaCe_{0.25}Mn_{0.75}O_{3-d}$	Pechini	3	1350/1000	40.0	Ar/wet Ar	82.0	140.0	[3]
$Sr_{0.75}Ce_{0.25}MnO_{3-d}$	Pechini	3	1350/800	40.0	Ar/wet Ar	68.0	98.0	[4]
$La_{0.6}Sr_{0.4}FeO_{3-d}$	commercial	5	1400/1400	45.0	N_2/wet N_2	327.2	124.0	[5]
$BaFeO_{3-d}$	sol-gel	9	900/900	30.0	Ar/wet Ar	Reduced by H_2	216.9	[6]

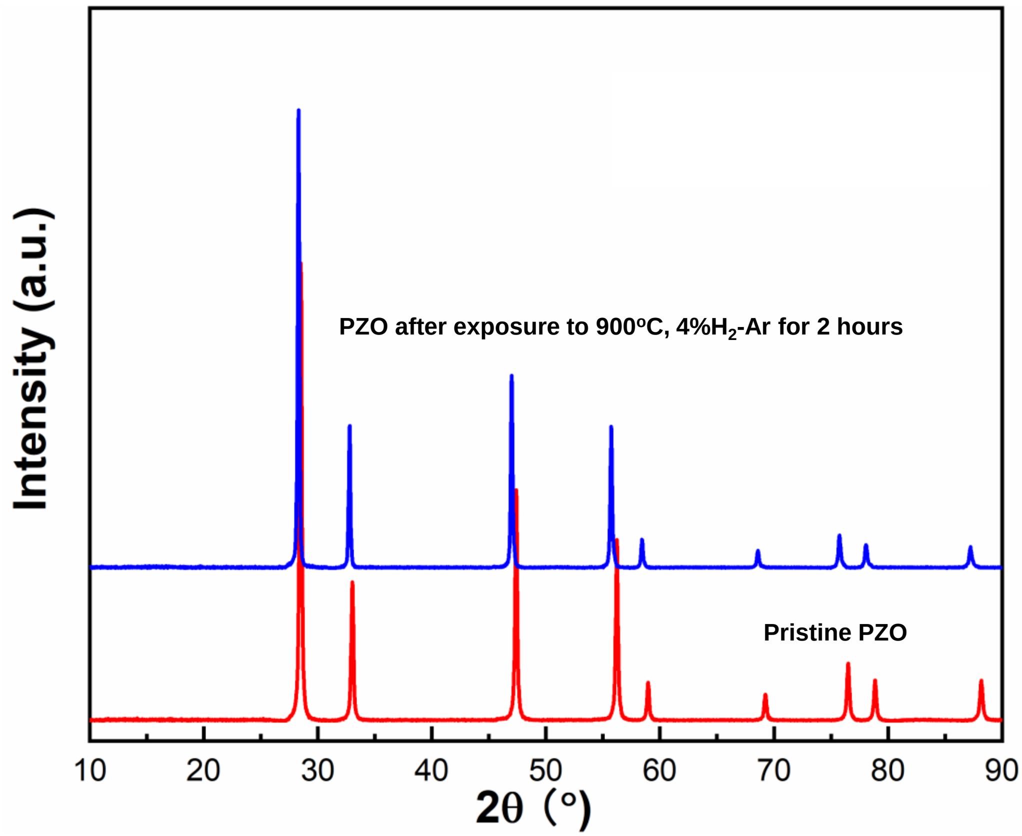

Figure S7. Comparison of XRD patterns of PZO before and after exposure to 4%H_2-Ar at 900ºC for 2 hours.

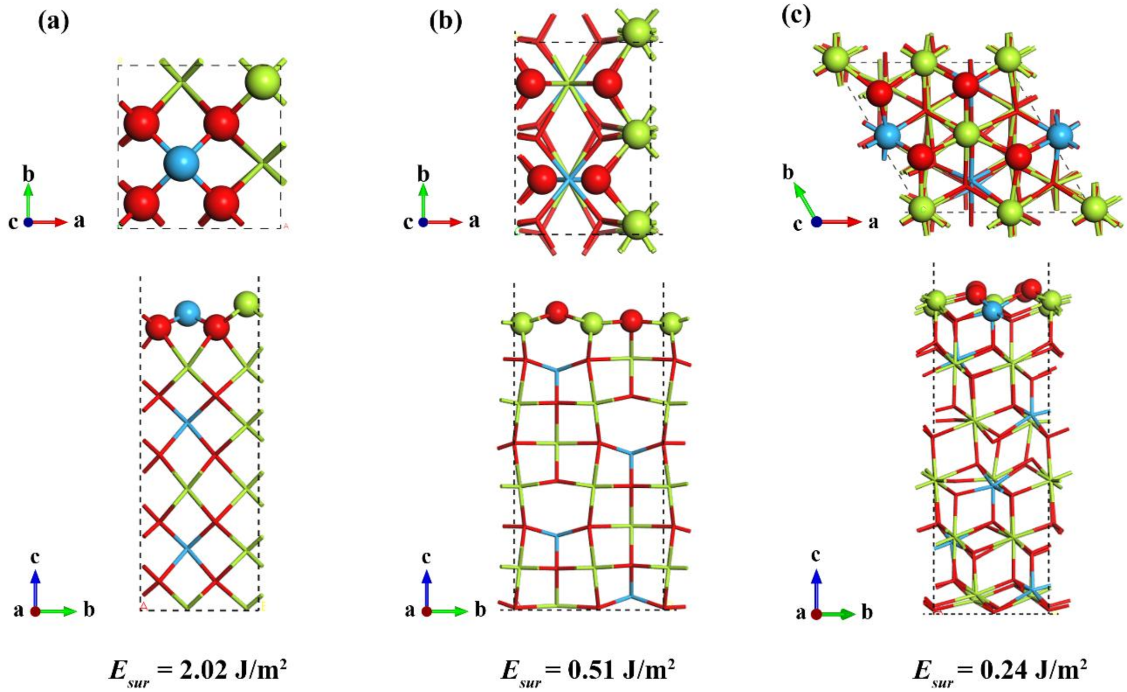

Figure S8. Top and side views of the PZO (100) (a), PZO (110) (b), and PZO (111) (c) surface models along with the surface formation energies. O, Pr, and Zr atoms are represented by red, green, and blue small balls, respectively. Atoms of the top layer are represented by small balls, while remaining atoms are represented by sticks.

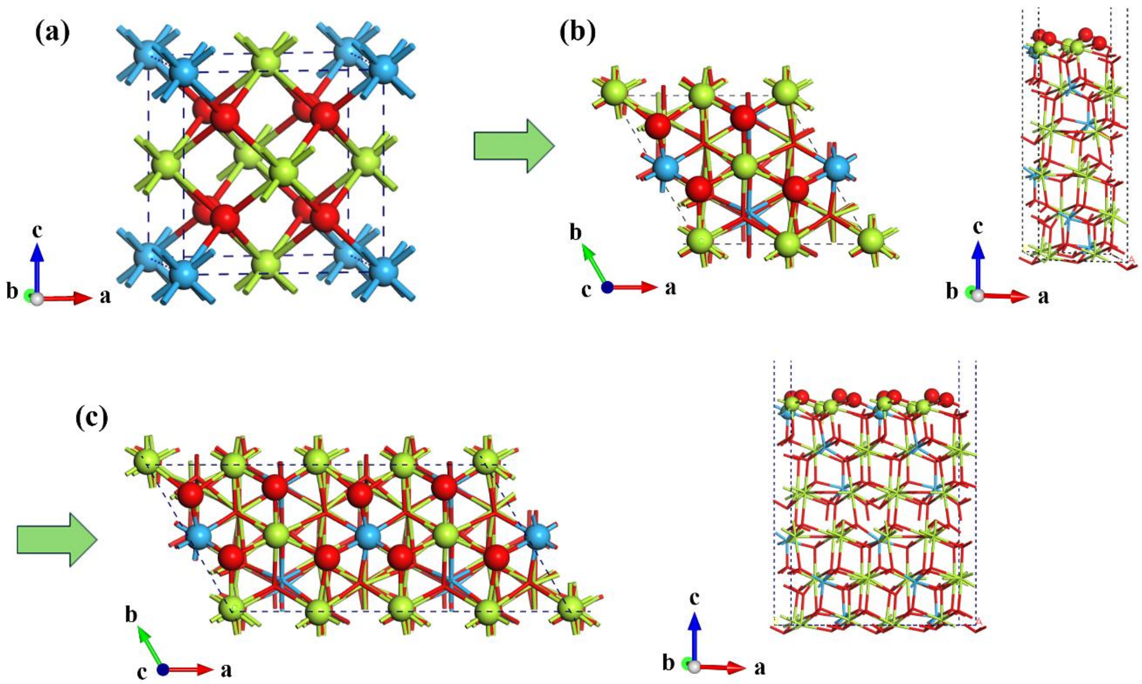

Figure S9. The PZO Unit cell (a); top and side views of the cleaved PZO (111) unit cell (b); top and side views of a 2×1×1 PZO (111) supercell (c). O, Pr, and Zr atoms are represented by red, green, and blue small balls, respectively. Atoms of the top layer are represented by small balls, while remaining atoms are represented by sticks.

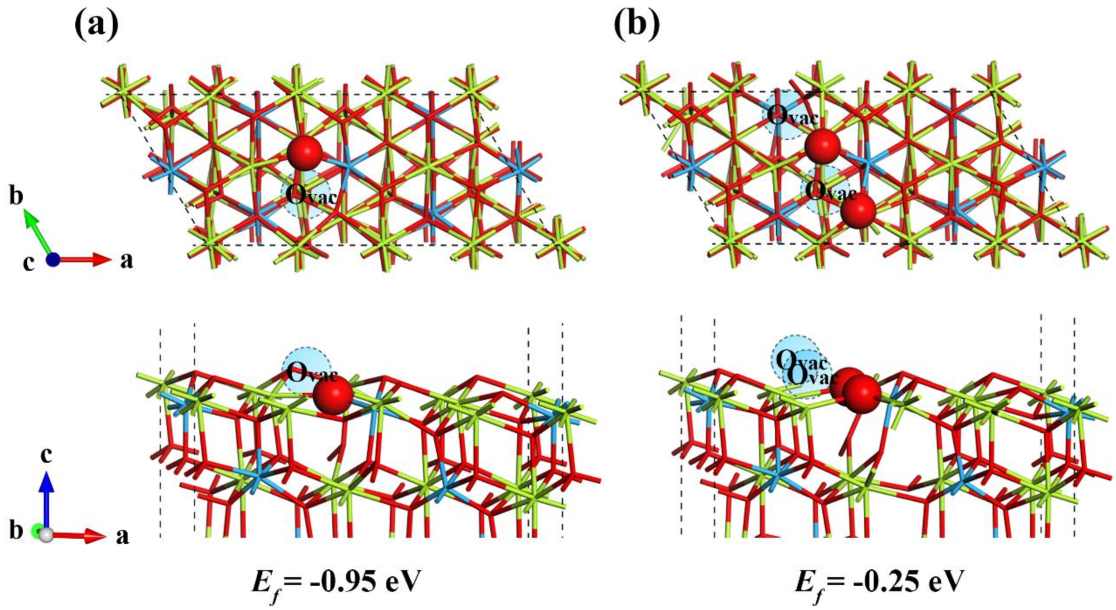

Figure S10. Top and side views of oxygen vacancies at various concentrations on the clean PZO (111) surface, along with the vacancy formation energies. The red balls represent oxygen atoms moving from the subsurface to the surface.

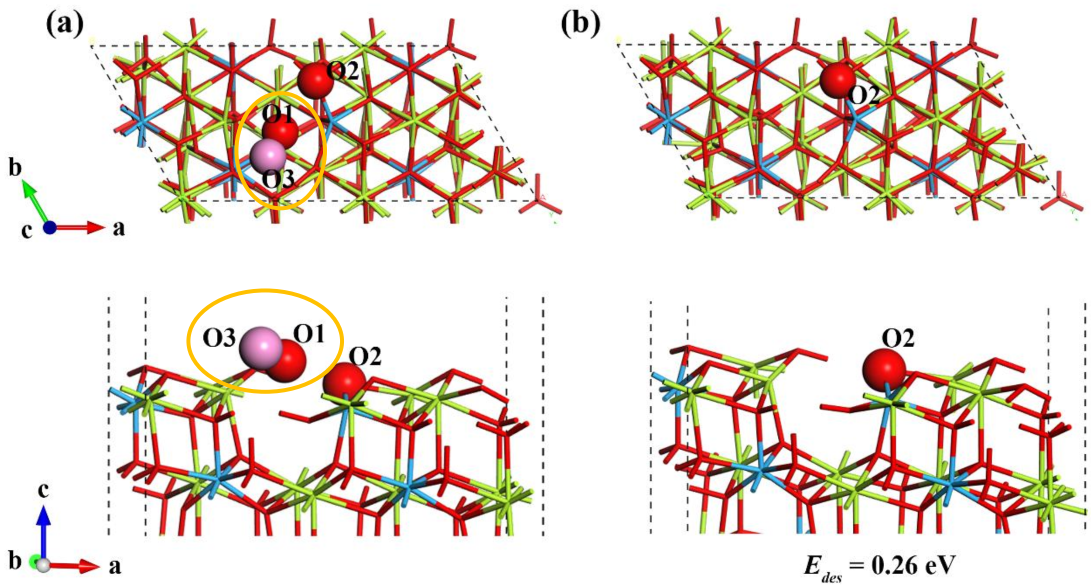

Figure S11. Schematic diagram of oxygen molecule desorption before (a) and after (b).

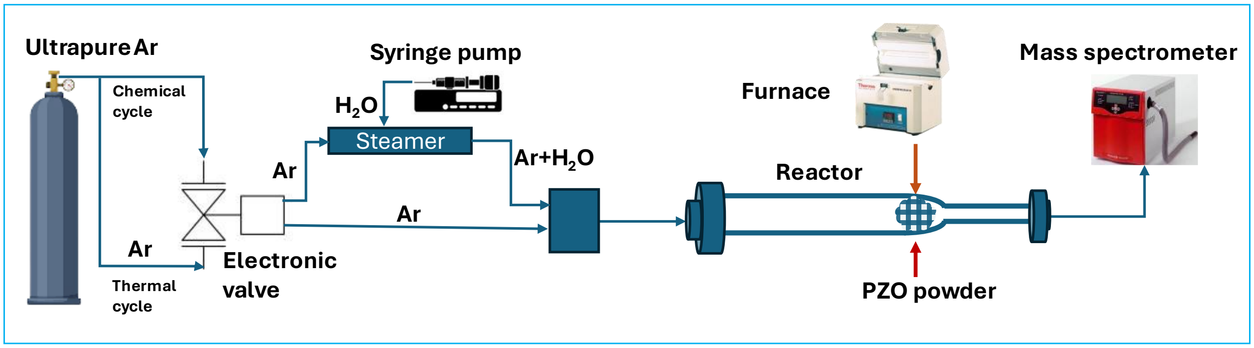

Figure S12. Experimental setup for TC performance evaluation.

References

1 Kaneko, H. *et al.* Reactive ceramics of CeO {sub 2}-MO {sub x}(M= Mn, Fe, Ni, Cu) for H {sub 2} generation by two-step water splitting using concentrated solar thermal energy. *Energy (Oxford)* **32** (2007).

2 Gokon, N. *et al.* Thermochemical two-step water splitting cycle using perovskite oxides based on LaSrMnO3 redox system for solar H2 production. *Thermochimica Acta* **680**, 178374 (2019).

3 Barcellos, D. R., Sanders, M. D., Tong, J., McDaniel, A. H. & O'Hayre, R. P. BaCe 0.25 Mn 0.75 O 3− δ—a promising perovskite-type oxide for solar thermochemical hydrogen production. *Energy & Environmental Science* **11**, 3256-3265 (2018).

4 Heo, S. J., Sanders, M., O'Hayre, R. & Zakutayev, A. Double-site substitution of Ce into (Ba, Sr) MnO3 perovskites for solar thermochemical hydrogen production. *ACS Energy Letters* **6**, 3037-3043 (2021).

5 Orfila, M. *et al.* Perovskite materials for hydrogen production by thermochemical water splitting. *International Journal of Hydrogen Energy* **41**, 19329-19338 (2016).

6 Ngoensawat, A., Tongnan, V., Laosiripojana, N., Kim-Lohsoontorn, P. & Hartley, U. Effect of La and Gd substitution in BaFeO3-δ perovskite structure on its catalytic performance for thermochemical water splitting. *Catalysis Communications* **135**, 105901 (2020).